

## RESEARCH ARTICLE

# Climbing parrots achieve pitch stability using forces and free moments produced by axial–appendicular couples

Lindsey L. Reader<sup>1,\*‡</sup>, David R. Carrier<sup>1</sup>, Franz Goller<sup>1</sup>, Michael R. Isaacs<sup>2</sup>, Alexis Moore Crisp<sup>3</sup>, Clinton J. Barnes<sup>2</sup> and David V. Lee<sup>2,\*</sup>

## ABSTRACT

During vertical climbing, the gravitational moment tends to pitch the animal's head away from the climbing surface and this may be countered by (1) applying a correcting torque at a discrete contact point, or (2) applying opposing horizontal forces at separate contact points to produce a free moment. We tested these potential strategies in small parrots with an experimental climbing apparatus imitating the fine branches and vines of their natural habitat. The birds climbed on a vertical ladder with four instrumented rungs that measured three-dimensional force and torque, representing the first measurements of multiple contacts from a climbing bird. The parrots ascend primarily by pulling themselves upward using the beak and feet. They resist the gravitational pitching moment with a free moment produced by horizontal force couples between the beak and feet during the first third of the stride and the tail and feet during the last third of the stride. The reaction torque from individual rungs did not counter, but exacerbated the gravitational pitching moment, which was countered entirely by the free moment. Possible climbing limitations were explored using two different rung radii, each with low and high friction surfaces. Rung torque was limited in the large-radius, low-friction condition; however, rung condition did not significantly influence the free moments produced. These findings have implications for our understanding of avian locomotor modules (i.e. coordinated actions of the head–neck, hindlimbs and tail), the use of force couples in vertical locomotion, and the evolution of associated structures.

**KEY WORDS:** Vertical, Branch, Dynamics, Torque, Gait, Locomotion

## INTRODUCTION

Specialization for scansorial locomotion appears in every class of terrestrial vertebrate and is implicated in a wide variety of ecological functions and evolutionary transitions (Hildebrand and Goslow, 2001). Despite its centrality to arboreality and its phylogenetic ubiquity, the full diversity of climbing styles and their underlying mechanisms are not well understood. Most mechanistic work has focused on two main types of arboreal locomotion: (1) small quadrupedal animals moving more-or-less horizontally on branches, where roll avoidance achieved by diagonal-sequence walking gaits has been of primary interest (Fischer et al., 2010; Lammers, 2009; Lammers and Biknevicius, 2004; Lammers and

Gauntner, 2008a; Shapiro and Young, 2012), and (2) vertical climbing by vertebrate taxa relying on various types of surface adhesion (e.g. Autumn et al., 2006; Jusufi et al., 2008; Zaaf et al., 2001a; Lammers and Sufka, 2013).


We consider vertical climbing to be on a surface within 20 deg of vertical. Hunt et al. (1996) define climbing to occur at angles within 45 deg of vertical to distinguish climbing from more horizontal arboreal locomotion, specifying 'vertical climbing' as within 10 deg of vertical and 'sub-vertical climbing' as 10–20 deg from vertical. Climbing animals minimize the distance between their center of mass (CoM) and the surface (Biewener, 2003; Bock and Winkler, 1978) and, assuming that this distance is, say, 20% of the lengthwise distance between support points, the gravitational moment will not pitch the animal away from the surface on a slope less than 68 deg (Fig. 1C). This principle can be demonstrated by placing a sanding block on a board and increasing the degree of inclination until it topples. Given that vertical and sub-vertical climbing are at angles greater than 70 deg, they include a pitching moment that tends to rotate the animal away from the climbing surface. This is because the CoM is sufficiently distant from the climbing surface that gravity causes the animal to pitch away from the substrate in the absence of an opposing moment (Biewener, 2003; Bock and Winkler, 1978; Cartmill, 1985). We would expect vertical climbers to be under particularly intense selection for their ability to dynamically control pitch rotation. Because the gravitational moment is proportional to the distance of the CoM from the climbing surface, climbing quadrupeds adjust their kinematics to keep their bodies close to the surface (Clemente et al., 2013) and tend to maintain simultaneous substrate contacts with multiple appendages (Biewener, 2003; Hildebrand and Goslow, 2001).

During vertical climbing, geckos (Autumn et al., 2006) and cockroaches (Goldman et al., 2006) have been shown to resist the gravitational pitching moment by pulling inward (toward the climbing surface) with their forelegs and pushing outward (away from the climbing surface) with their hindlegs, thus producing a free moment that tends to rotate the head toward the climbing surface. The tails of geckos push against the substrate as an emergency response to slippage but do not contribute to the free moment during unperturbed vertical climbing (Jusufi et al., 2008).

Quadrupeds that climb vertically generally have palmigrade postures (effectively reducing limb length) or flattened digits (increasing the surface area in contact with the substrate; Hildebrand and Goslow, 2001) and are smaller than their terrestrial counterparts (Biewener, 2003). Scansorial lizards tend to be dorsoventrally flattened compared with more terrestrial species (Zaaf et al., 2001a,b) and have relatively shorter limbs (Hagey et al., 2017). Some have shortened proximal segments of both the forelimb and the hindlimb, which could reduce the effective limb length (Hagey et al., 2017). Tulli et al. (2011) saw only longer humerus lengths in clinging lizards compared with their climbing relatives. Truly

<sup>1</sup>Department of Biology, 201 South Biology Building, University of Utah, Salt Lake City, UT 84112, USA. <sup>2</sup>School of Life Sciences, 4505 S. Maryland Parkway, University of Nevada Las Vegas, Las Vegas, NV 89154, USA. <sup>3</sup>Iadarola Center, Room 204, Cabrini University, 610 King of Prussia Road, Radnor, PA 19087, USA. \*These authors contributed equally to this work

‡Author for correspondence (l.reader@utah.edu)

 L.L.R., 0000-0002-5219-501X; C.J.B., 0000-0002-9627-9653

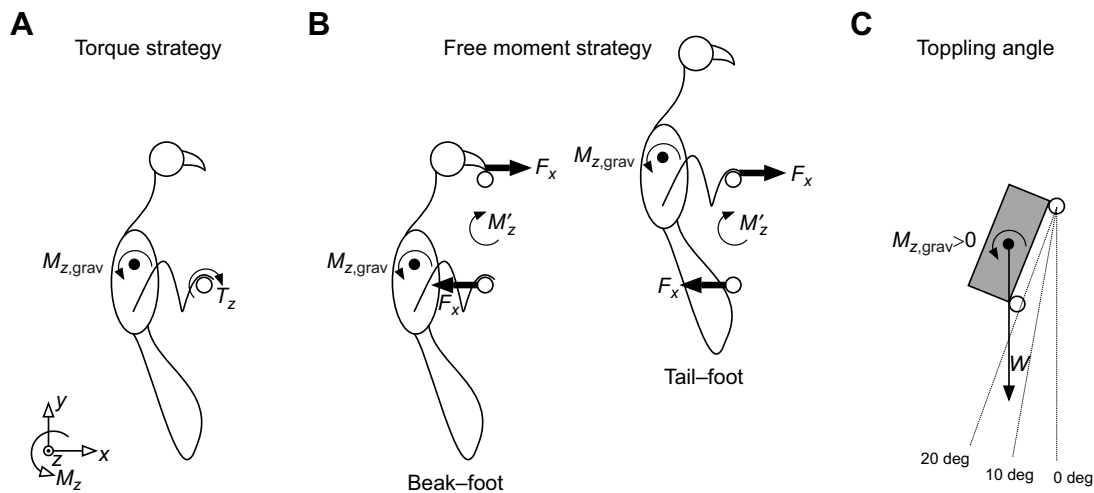


**Fig. 1. Two possible mechanisms for exerting pitching moments during vertical climbing.** In a given stride,  $M_{z,grav}$  is determined by the average distance of the center of mass (CoM) from the climbing surface and is positive in the coordinate system used here. (A) In the torque strategy,  $M_{z,grav}$  is resisted by a torque  $T_z$  provided by a grasping or adhesive appendage such as a foot, or possibly by a grasping beak for some species. (B) In the free moment strategy,  $M_{z,grav}$  is resisted by opposing horizontal forces ( $F_x$ ) on separate rungs, which produce a free moment  $M_z'$ . In order to counter the gravitational moment, the upper point of contact must pull toward the rung and the lower point of contact must push away from the rung, such that  $M_z'$  is negative. (C) Toppling angle is around 22 deg when the distance of the CoM from the climbing surface is 20% the lengthwise distance between contact points. Weight,  $W=mg$ .

scansorial mammals (i.e. vertical/near-vertical climbers, not brachiators, branch walkers or leapers) show shorter femur lengths relative to humerus lengths, a pattern repeated in a diverse range of taxa, including koalas, some opossums and porcupines (Godfrey et al., 1995; mustelids: Heinrich and Biknevicius, 1998; lorises: Runestad, 1997). This has been loosely hypothesized as a mechanism of straightening the hindlimb so that the femur better aligns with reaction forces (Heinrich and Biknevicius, 1998) and/or reducing the gravitational pitching moment when climbing by bringing the CoM closer to the substrate (Heinrich and Biknevicius, 1998; Runestad, 1997).

Scansorial birds generally have shorter legs (Richardson, 1942) and tarsometatarsi (Stoessel et al., 2013; Zeffner and Norberg, 2003; Zeffner et al., 2003) than terrestrial taxa; and tarsometatarsus length has been found to be a strong ecological signal across birds in general (Zeffner et al., 2003). Specialized bark foragers also have shortened tibiotarsi (Richardson, 1942), which is the segment that may contribute most to effective leg length, thereby decreasing the gravitational pitching moment. Differences in muscle origin and insertion sites of the hip and ankle flexors point to greater mechanical advantage about the hip and ankle joints in climbers, as do generally less-developed extensor muscles and longer tendinous loops that facilitate more direct lines of muscle action (Richardson, 1942).

Effective climbing is clearly seen across multiple avian clades, and two orders – Piciformes (woodpeckers) and Psittaciformes (parrots) – are almost exclusively composed of climbing specialists (Fujita et al., 2007, 2008; Hildebrand and Goslow, 2001; Norberg, 1986; Richardson, 1942; Spring, 1965). Many small-bodied passerines are capable of climbing and/or clinging to some extent, including upside-down on overhanging branches (Carrascal et al., 1990; Moreno and Carrascal, 1993). The woodpeckers (Piciformes: Picidae), woodcreepers (Passeriformes: Furnariidae), nuthatches (Passeriformes: Sittidae) and treecreepers (Passeriformes: Certhiidae) are tree trunk climbing specialists. Parrots (Psittaciformes, three families) are grasping climbers, generally using slender branches or vines rather than continuous climbing surfaces such as trunks, often with the aid of their beaks and necks. All members of the order

Piciformes seem to be able to climb using this strategy, regardless of mass (11 g to nearly 4 kg: Dunning, 2008) or foraging style (flightless and ground dwelling to canopy specialists: Forshaw and Knight, 2010). The pygmy parrots (*Micropsitta* spp.) retain grasping capabilities, but are specialized trunk foragers whose general morphology converges with that of nuthatches and treecreepers.

Parrots exhibit many morphological features that are interpreted as general adaptations to climbing (Hildebrand and Goslow, 2001; Sustaita et al., 2013), and can be divided by functionality into those that facilitate grasping and those that facilitate both a long reach and flexibility of the legs and neck. Features that enable grasping include long opposing digits, a rounding of interdigital articular surfaces, as well as tarsometatarsal and digital pads that are cushioned, textured and tactilely sensitive. Psittacine-specific features that enable reach and/or flexibility are a long neck and a relatively large range of motion in most hindlimb joints. Both the gravitational pitching moment encountered in arboreal habitats and the dexterity required for foraging by most parrots might favor relatively shorter hindlimbs, and parrots are known to have shorter tarsometatarsi than other taxa (Stoessel et al., 2013; Zeffner and Norberg, 2003; Zeffner et al., 2003).

Here, we hypothesize that vertical climbing in parrots could be facilitated by two main mechanisms for opposing the gravitational pitching moment: (1) grasping and twisting by the feet and possibly by a grasping beak and (2) exerting opposing forces normal to the climbing surface with the beak, feet and tail at spatially separated points of contact. The first mechanism relies on application of torque about the climbing rung in an orientation that would counteract the pitching moment – we call this the torque strategy (Fig. 1A). The second mechanism relies on points of contact separated by some distance, such as between surfaces being grasped (e.g. branches, vines or bark), to apply a force couple. A force couple is a pair of equal and opposite forces with parallel lines of action separated by some distance. By definition, the forces sum to zero in a force couple and there is a free moment (i.e. a moment that does not depend on the point of force application with respect to the CoM) equal to the product of the force magnitude and the distance

between the lines of action of the forces in the couple – we call this the free moment strategy (Fig. 1B). Even when opposing normal forces are unequal, their net effect can be represented by a free moment determined by using the force of lesser magnitude in the force couple. The free moment of a rigid body does not have any defined point of application because it does not represent a net force that would exert a torque about the CoM (e.g. Holden and Cavanagh, 1991). We stress that the torque strategy and the free moment strategy are not mutually exclusive mechanisms and could be employed at different points in the stride cycle or even simultaneously.

The coefficient of friction between any morphological point of contact and the climbing surface is a potential limitation for both the torque strategy and the free moment strategy. However, friction limitations may be overcome by exerting a greater grasping force normal to the circumference of the rung and/or by wrapping the digits around the rung more completely. In the case of the ladder rung configuration used in this study, friction may limit the torque that can be applied about the rung axis ( $T_z$ ) and also the forces perpendicular to the rung's long axis ( $F_x, F_y$ ), as per the coordinate system of Fig. 1. In addition, the grasping force should be constrained by the circumference of the climbing rung relative to the length of the foot (or the beak, if used for grasping). Based on this same principle, large-radius tree trunks preclude high grasping forces in lemurs that grasp using both forelimbs (Johnson et al., 2015). During quadrupedal branch walking, opossums use longer stance contact times and equalize medial forces to compensate for frictional force limitations on branches that are too large to grasp completely with a single hand/foot (Lammers and Biknevicius, 2004). Torque about cylindrical grips is rarely measured (Lammers and Gauntner, 2008a), but was found to counter rolling moments experienced by branch-walking quadrupeds (Lammers and Gauntner, 2008b).

Here, we used a climbing ladder with individually instrumented rungs to measure reaction force and torque during vertical climbing of small parrots (green-cheeked conures, *Pyrrhura molinae*) and uncover basic climbing mechanisms, including strategies used to resist the gravitational pitching moment. The effects of rung radius and surface friction were investigated to probe any limitations imposed by these conditions. We measured climbing mechanics across four combinations of rung radius and surface friction conditions, reporting spatiotemporal parameters, as well as forces and moments during complete climbing strides.

## MATERIALS AND METHODS

### Selection and care of animals

We selected green-cheeked conures, *Pyrrhura molinae* Massena and Soutance 1854 – small arboreal parrots native to the Amazon basin (Forshaw and Knight, 2010) – as representative avian climbers. They are readily available in the pet trade and small enough to climb naturally in the X-ray view. Three young adult conures (one male and two females, aged 1–2 years) were socialized extensively and trained for the climbing trials (Table 1). All were housed at the University of Utah with free-choice food and water until the time of the experiments; they were then transported to the

University of Nevada, Las Vegas, and housed in the same conditions throughout the experimental time frame. All housing and travel were conducted in accordance with the requirements of the Animal Care and Use Committees of the University of Utah (Protocol #12-02006) and the University of Nevada, Las Vegas (Protocol #R0310-252) and a Memorandum of Understanding between the two universities.

### Experimental setup

We constructed a ladder rail angled at 9.5 deg to the vertical using T-slot aluminium, onto which four 6-axis force–torque transducers (Nano17, ATI Industrial Automation, Apex, NC, USA) were mounted via a 3D-printed housing of ABS plastic (Fig. 2). 3D-printed rungs of two different radii could then be easily installed onto the sensing end of the cylindrical transducers. Two sets of four cylindrical ladder rungs were 3D printed with ABS plastic (Makerbot Replicator™ 2012). The rungs were 65 mm long with one set having a radius of 4.25 mm and circumference approximately equal to the parrots' foot span, referred to as the small-radius condition 'r'. The large-radius condition 'R' used rungs of the same length with a radius of 8.5 mm, and a circumference roughly twice the parrots' foot span. The rungs were first installed unaltered, having only slight texturing due to 3D printing (termed low-friction 'f') and then coated with liquid electrical tape to increase the friction coefficient between the foot and the rung surface (termed high-friction 'F').

In all climbing trials, rungs were spaced 100 mm apart (center-to-center), which was determined empirically to be a comfortable distance for all birds to achieve steady-state climbing. We angled the ladder 9.5 deg from the vertical to prevent visual overlap of the rungs in the vertical X-ray view and also oriented it obliquely with respect to the horizontal X-ray view to provide a clear view of interactions with the rungs. In each trial, we recorded two full stride cycles, centered on the second and third rungs of the four-rung series. The strides centered on the second and third rungs are referred to here as the first and second strides, respectively. To help initiate and maintain smooth climbing, we placed a non-instrumented, slightly unstable branch below and offset from the first instrumented rung, and a branch containing an apple slice above the last instrumented rung (Fig. 2). Any open spaces around the climbing apparatus were walled off with Styrofoam, with a small hinged door cut out for easy release and retrieval of the birds.

### Experimental methods

All climbing trials were filmed in orthogonal X-ray planes (horizontal and vertical) to allow for 3D tracking of anatomical landmarks for future analysis. The X-ray sources were energized at 78 kV<sub>cp</sub> and 5 mA. X-ray images were captured with two adjustable zoom 40 cm image intensifiers (Medex QXS-164) using a 30 cm zoom setting, coupled to two high-speed digital video cameras (Phantom Miro 4; 12-bit, monochrome) recording at 250 frames s<sup>-1</sup>. Three-dimensional force and torque were measured by six-axis ATI Nano17 transducers supporting each instrumented rung of the climbing ladder (Fig. 2). The z-axis of each transducer was aligned with its corresponding ladder rung, defining the lateral

**Table 1. Mass and morphometrics**

Mass (g)	Foot span (mm)		Length (mm)						
	Long arc	Short arc	Beak	Femur	Tbt	Tmt	Body+tail	Trunk	Head+neck+beak
62.33±3.40	39.1	22.9	22.4	22.5	37.9	16.4	210	61	64.1

Mass data are means±s.d. Tbt, tibiotarsus; Tmt, tarsometatarsus.

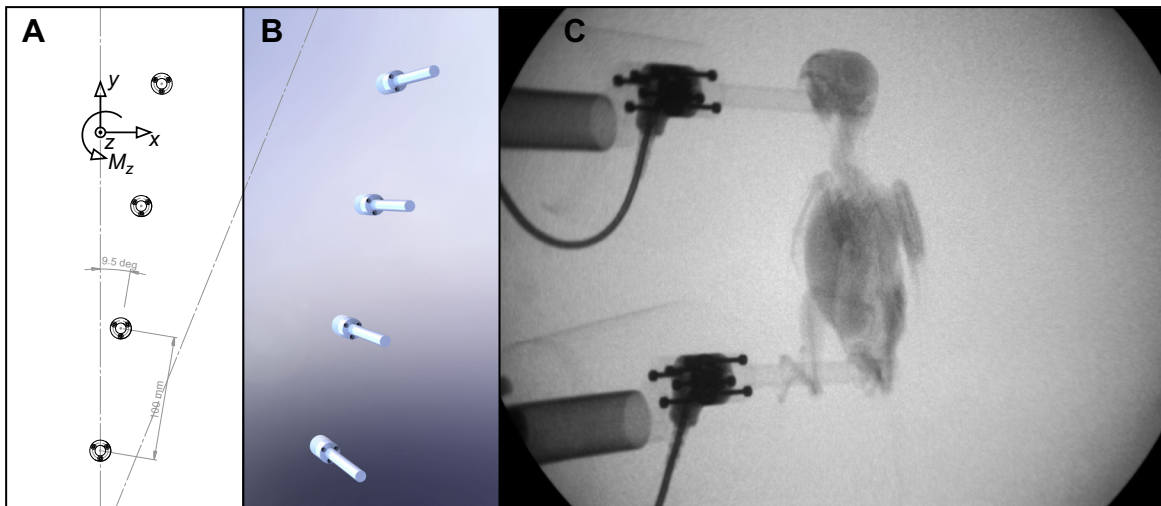


**Fig. 2. Rung design, placement and spacing.** In the experimental climbing apparatus, rungs were spaced 100 mm from the center of one rung to the center of the next rung and the ladder was angled at 9.5 deg from the vertical (A), as rendered for the small-radius rungs attached to the force–torque transducers (B). (C) A green-cheeked conure initiating a stride on the central rungs of the ladder, as seen in horizontal X-ray view.

axis. The  $y$ -axis was aligned with the ladder rail (i.e. the plane of the climbing ladder), so we rotated the coordinate system 9.5 deg about the  $z$ -axis such that force in the  $y$ -axis is vertical and force in the  $x$ -axis is horizontal (Fig. 2B). Force and torque data were recorded with eight National Instruments NI-9237 4-channel strain-bridge amplifier modules in a cDAQ-9188XT chassis using LabView 2013. Transducer data were synchronized to X-ray kinematics by receiving a 5 V TTL post-trigger from the Miro 4 cameras upon capture of the final X-ray video frame.

Birds were weighed on a digital bench top scale before each data collection session and for one bird, post-mortem measurements of hindlimb segments were made to the nearest 0.1 mm using digital calipers (Table 1). Long-arc measurements spanned the length of the lateral (longest) pair of opposing toes. Short-arc measurements spanned the length of the medial (shortest) pair of toes.

For each trial, a handler placed an individual bird into the X-ray through the Styrofoam door. Once the handler was outside of the X-ray vicinity, we turned on the X-ray sources and a LED light located inside the X-ray enclosure, which encouraged the bird to begin climbing. After completing the climb, the bird was retrieved by the handler and allowed to socialize until the next trial. Data collection was completed over multiple days for each of the four rung conditions to be tested sequentially (small-radius, low-friction: ‘rF’; small-radius, high-friction: ‘rF’; large-radius, low-friction: ‘RF’; large-radius, high-friction: ‘RF’). Birds completed the small-radius trials before the large-radius trials because this change required removal and reattachment of rungs to the transducers. High-friction trials were always conducted after low-friction trials because the liquid electrical tape was then permanently applied to the same 3D-printed rungs.

### Analysis

Strides selected for analysis were smoothly executed at a consistent speed with no turning or repositioning of limbs on a given rung. We used initial contact phases and duty factors to quantify the gait used for climbing under the four different experimental rung conditions (Table 2). Only the two complete strides occurring nearest to the center of the ladder were analyzed. The first stride spans instrumented rungs 1–3, and the second stride spans instrumented rungs 2–4. The stride period was defined from

initial beak contact on one rung to initial beak contact on the next rung. Contact and departure times were determined from the X-ray video and reaction force patterns. Spatiotemporal, force, torque and free moment parameters were calculated in LabView 2013 for the whole stride and individual rungs during the stride (Table 2). We manually set six cursors to mark the timing of stride events, chronologically: ‘Begin-stride’ at the initial beak contact on the upper rung; ‘Begin-foot 1’ at the initial contact of the first foot on the upper rung; ‘End-foot 2’ at the departure of the second foot from the lower rung; ‘Begin-tail’ at the initial contact of the tail on the lower rung; ‘Begin-foot 2’ at the initial contact of the second foot on the upper rung; and ‘End-stride’ at the initial beak contact on the subsequent rung.

Reaction forces were normalized by body weight (BW). The three birds were of similar size, so torques and moments were simply normalized by BW. The calculation of the free moment about the pitch axis ( $M_z'$ ) is simplified by the regular spacing of ladder rungs because the center of pressure is restricted to a point within the circumference of the cylindrical rung. We subtracted 6 mm from the vertical distance between rungs to account for a potentially eccentric center of pressure biased toward the bottom and top of adjacent rungs, thereby providing a conservative estimate of  $M_z'$ . Free moment is the product of this adjusted vertical distance ( $S'$ ) between rungs and the horizontal force of least magnitude (because opposing forces must be equal in magnitude) in the force couple ( $F_x'$ ) (Table 2). The free moment is only calculated in instances where horizontal forces between adjacent rungs are of opposite sign because there is no free moment when they act in the same direction. The direction of the free moment is determined by the sense of rotation of the force couple, which follows the convention diagrammed in Fig. 1.

### Statistics

We used generalized linear mixed models in JMP Pro (1989–2007, SAS Institute Inc., Cary, NC, USA) to analyze spatiotemporal and kinetic parameters across the categorical effects of each of the four radius/friction combinations (Condition), lower versus upper rung (Rung), and first versus second stride (Stride). Interactions were assessed for factors exhibiting significant differences and Tukey *post hoc* corrections were conducted for factors or interactions with

**Table 2. Definitions of spatiotemporal and kinetic parameters**

Parameter	Units	Definition
$T$	s	Stride period defined from initial beak contact at one rung to initial beak contact at the next rung
$L$	mm	Stride length, equal to the distance between subsequent climbing rungs (100 mm)
$\bar{V} = L/T$	mm s <sup>-1</sup>	Mean climbing speed during the stride period
$\alpha$	deg	Angle of the climbing ladder with respect to the vertical (9.5 deg)
$S = L \cos \alpha$	mm	Vertical distance between rungs
$\psi_{r1} = t_{0,r1}/T$		Phase of the first foot's initial contact ( $t_{0,r1}$ ) with respect to initial beak contact at the beginning of the stride
$\psi_{r2} = t_{0,r2}/T$		Phase of the second foot's initial contact ( $t_{0,r2}$ ) with respect to initial beak contact at the beginning of the stride
$\psi_{tail} = t_{0,tail}/T$		Phase of the tail's initial contact ( $t_{0,tail}$ ) with respect to initial beak contact at the beginning of the stride
$DF = t_{beak}/T$		Duty factor of the beak, where $t_{beak}$ is the duration of beak contact in seconds
$DF = t_{f1}/T$		Duty factor of the first foot, where $t_{f1}$ is the duration of the first foot's contact in seconds
$DF = t_{f2}/T$		Duty factor of the second foot, where $t_{f2}$ is the duration of the second foot's contact in seconds
$F_x$	N	Horizontal reaction force perpendicular to the rung axis (positive force tends to move the bird toward the rung)
$F_y$	N	Vertical reaction force (positive force tends to move the bird upward)
$F_z$	N	Lateral reaction force (positive force tends to move the bird rightward)
$T_z$	N mm	Reaction torque about the rung (z-axis) (positive torque tends to pitch the bird's nose away from the climbing ladder)
$M'_z = F'_x S'$	N mm	Free moment acting on the body about the z-axis, i.e. pitching due to equal and opposite $F_x$ on separate rungs, where a positive free moment pitches the bird's nose away from the climbing ladder <ul style="list-style-type: none"> <li>the vertical distance between subsequent rungs (<math>S</math>) is reduced by 6 mm to account for eccentric contact points that may shorten this distance – conservatively, estimating a minimum vertical distance <math>S' = 92</math> mm between contacts on subsequent rungs</li> <li><math>M'_z</math> is only calculated if <math>F_x</math> is opposite on subsequent rungs in a given instance; if <math>F_x</math> is in the same direction, <math>M'_z = 0</math></li> <li><math>M'_z</math> is calculated based upon the <math>F_x</math> of lesser magnitude (<math>F'_x</math>) on the lower and upper rung in given instance of the stride</li> </ul>
$\bar{F}_x = \int_0^T F_x dt / Tmg$	BW	Mean horizontal reaction force as a fraction of body weight
$ \bar{F}_x  = \frac{ \bar{F}_{x,lower}  +  \bar{F}_{x,upper} }{2mg}$	BW	Mean magnitude of horizontal reaction force on the upper and lower rungs, as a fraction of body weight
$\bar{F}_y = \int_0^T F_y dt / Tmg$	BW	Mean vertical reaction force as a fraction of body weight
$\bar{F}_z = \int_0^T F_z dt / Tmg$	BW	Mean lateral reaction force as a fraction of body weight
$\bar{\tau}_z = \int_0^T \tau_z dt / Tmg$	BW mm	Mean reaction torque about the z-axis as a fraction of body weight
$\bar{M}'_z = \int_0^T M'_z dt / Tmg$	BW mm	Mean free moment about the z-axis as a fraction of body weight

more than two levels (Tables S1 and S2). Relationships between the mean free moment ( $M'_z$ ) and the mean magnitude of horizontal force ( $|\bar{F}_x|$ ) were further analyzed by standard major axis (SMA) regression, comparing slopes across experimental conditions using the *smatr* package in *R*. In all analyses, Subject was included as a random factor to account for potential variation between individuals.

## RESULTS

### Climbing gait

Conures lead the gait cycle by extending the neck and placing the tip of the beak on the top of the subsequent or 'upper' rung, but do not grasp the rung with their beak as is often seen in larger parrots (Movies 1–3). Beak contact is followed by contact of the first foot on the upper rung, which roughly coincides with lifting of the beak from the upper rung (Table 3, Fig. 3). In the second half of the stride, the second foot contacts the upper rung and the tail contacts the

lower rung. The beak occasionally skipped a rung, if the bird was traveling quickly enough, and these trials were excluded from the analysis.

The birds climbed more slowly ( $P < 0.0001$ ) on the large-radius, low-friction 'Rf' rungs compared with the other experimental rung conditions, where they climbed 8% faster on average. Because stride length was fixed by rung spacing, slower climbing speeds also represented longer stride periods in the Rf condition (Table 3; Table S1A).

The basic gait sequence did not change with respect to experimental rung conditions, yet the relative phases of foot and tail contact were adjusted, as were duty factors of the beak and feet (Table 3; Table S1B,C). These changes led to marked differences in the degree of temporal overlap between beak, foot and tail contacts in the Rf condition compared with the other three conditions (Fig. 3). For all conditions, there was some degree of overlap between the beak, foot and tail contacts; however, only the Rf

**Table 3. Mean ( $\pm$ s.d.) spatiotemporal gait parameters by experimental rung condition**

Condition	Stride period (s)	Duty factor			Contact phase			
		Beak	Foot 1	Foot 2	Beak	Foot 1	Foot 2	Tail
rf ( $n=18$ )	0.653 $\pm$ 0.183	0.354 $\pm$ 0.084	0.732 $\pm$ 0.084	0.672 $\pm$ 0.060	0	0.330 $\pm$ 0.083	0.783 $\pm$ 0.115	0.582 $\pm$ 0.119
rF ( $n=21$ )	0.727 $\pm$ 0.137	0.345 $\pm$ 0.072	0.680 $\pm$ 0.099	0.635 $\pm$ 0.095	0	0.319 $\pm$ 0.078	0.754 $\pm$ 0.116	0.584 $\pm$ 0.133
Rf ( $n=12$ )	1.161 $\pm$ 0.403	0.602 $\pm$ 0.137	0.829 $\pm$ 0.087	0.729 $\pm$ 0.124	0	0.276 $\pm$ 0.079	0.508 $\pm$ 0.080	0.488 $\pm$ 0.164
RF ( $n=19$ )	0.774 $\pm$ 0.155	0.407 $\pm$ 0.082	0.770 $\pm$ 0.082	0.717 $\pm$ 0.109	0	0.296 $\pm$ 0.064	0.726 $\pm$ 0.101	0.566 $\pm$ 0.127

rf, small-radius, low-friction; rF, small-radius, high-friction; Rf, large-radius, low-friction; RF, large-radius, high-friction.

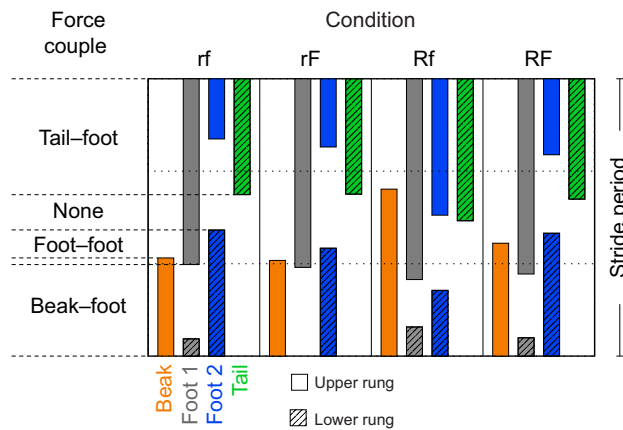


**Fig. 3. Gait pattern by experimental condition.** Mean phases of initial contact and duty factors are used to reconstruct contacts for a single stride period. Beak contact (orange) on the upper rung initiates the stride while both hindlimbs remain on the lower rung. Beak contact is followed by contact of foot 1 (gray) and foot 2 (blue) on the upper rung. The tail contacts the lower rung as foot 2 reaches for the upper rung and its contact period is arbitrarily drawn to the end of the stride because departure of the tail feathers could not be accurately visualized in the X-ray video. Dashed lines bracket periods where force couples between appendages on upper and lower rungs are possible. Cross-hatching indicates lower rung contacts. Condition: rf, small-radius, low-friction; rF, small-radius, high-friction; Rf, large-radius, low-friction; RF, large-radius, high-friction.

condition included a brief simultaneous contact of all four appendages during mid-stride. Duty factor for the beak increased in the Rf condition compared with the other three conditions ( $P < 0.0001$ ; Table S1B). Overall, the Rf condition seemed most difficult for the birds to execute, as slipping and readjustments were seen more often.

The relative phase of initial contact of the second foot decreased in the Rf condition, indicating earlier onset compared with the other three conditions (Table S1C). Likewise, initial contact of the tail occurred earlier in the Rf condition than in the small-radius conditions but was more similar to the large-radius, high-friction 'RF' condition (Table S1C). Overall, appendages contacted earlier and tended to stay in contact for a greater fraction of the stride period in the Rf condition. The hindlimb contacts are roughly half a cycle out of phase in all but the Rf condition, where the second foot makes contact less than a quarter of a cycle after the first foot. From the perspective of hindlimb contacts, the Rf gait might be called asymmetrical shuffling, while the gait used in the other three conditions is symmetrical bipedal striding with additional contacts of the beak and tail (Fig. 3).

### Rung reaction forces

Vertical reaction forces ( $F_y$ ) were distributed unequally between lower and upper rungs during a climbing stride cycle. Determined over the complete stride period (Table 2), mean vertical force was about 20% BW on the lower rung and 80% BW on the upper rung (Fig. 4A). This result indicates that most of the reaction force opposing gravity is due to the legs and/or beak pulling the bird upward from the upper rung instead of the legs pushing the bird upward from the lower rung. Note that it was not possible to distinguish individual limb forces, only their net contributions on respective rungs. The difference between lower and upper rungs (i.e. the main effect Rung), was highly significant ( $P < 0.0001$ ), and the random effect Bird was also significant ( $P = 0.0011$ ). However, the main effect Condition was not significant ( $P = 0.9754$ ), indicating

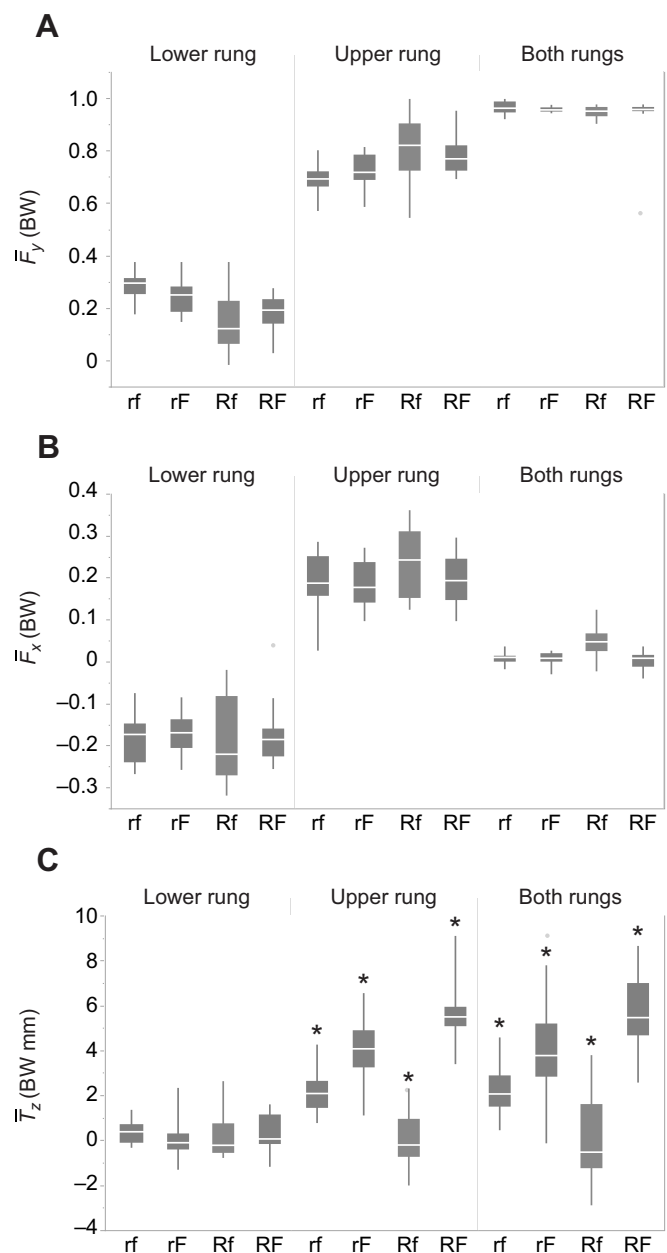


**Fig. 4. Mean reaction force and torque from the lower rung, upper rung and the two rungs combined.** (A,B) Mean vertical ( $F_y$ ; A) and horizontal ( $F_x$ ; B) reaction force determined over a full stride period. (C) Mean reaction torque about the long (i.e. pitch) axis of the rung ( $T_z$ ) determined over the full stride period. Force is in units of body weight (BW) and torque is in units of body weight millimeters (BW mm). Condition: rf, small-radius, low-friction; rF, small-radius, high-friction; Rf, large-radius, low-friction; RF, large-radius, high-friction. \*Significant pairwise difference ( $P < 0.05$ ) from other conditions (Table S1G,H). Rung: lower, upper, both.

similar mean vertical forces across conditions (Fig. 4A). The summed vertical reaction force from the lower and upper rungs was slightly less than 1 BW during the stride period (Fig. 4A), indicating a modest downward acceleration, i.e. a tendency for gradual slowing during vertical ascent of the ladder.

Horizontal reaction forces ( $F_x$ ) on separate rungs were approximately equal and opposite during climbing. During the climbing stride, a mean horizontal reaction force of about 20% BW pulls the bird toward the ladder at the upper rung, and a reaction force of equal magnitude pushes the bird away from the ladder at the

lower rung (Fig. 4B). The main effect Rung was highly significant ( $P<0.0001$ ), and Condition was also significant ( $P=0.0079$ ; Table S1D). Pairwise comparisons are provided for the two rungs combined because the interaction Rung $\times$ Condition was not significant ( $P=0.225$ ). Summing the horizontal forces of the lower and upper rung resulted in a net horizontal force near zero for all but the Rf condition, which showed a slight positive net force pulling the bird toward the climbing ladder.

### Reaction torque about the rung axis

Reaction torque about the long axis of the rung ( $T_z$ ) is the opposite of the torque exerted about the rung's long axis and may be a response to either perpendicular force ( $F_x, F_y$ ) applied eccentrically or a 'twisting' moment achieved by a grasping appendage(s) with at least two points of contact on the circumference of the rung. In the latter case, a negative reaction torque would indicate a free moment resisting the gravitational pitching moment (e.g. Fig. 1A), whereas a positive reaction torque would indicate a moment exacerbating the gravitational pitching moment. Mean  $T_z$  over the complete stride was positive across all conditions (Fig. 4C); hence, whether a result of eccentric perpendicular force or a twisting moment, the measured reaction torque cannot represent a moment resisting the gravitational pitching moment (Fig. 4C). In the measurement of reaction torque, there is unfortunately no direct method for distinguishing whether the torque exerted about the long axis of the rung is due to eccentric force or a twisting moment, except when there is a single focused contact point on the rung's circumference and twisting can be excluded, or in instances where the net perpendicular force is zero.

The main effect Rung was highly significant ( $P<0.0001$ ), with the lower rung showing torques that were significantly lower (approaching zero) than those of the upper rung (Fig. 4C). The main effect Condition was also highly significant ( $P<0.0001$ ), as was the interaction Rung $\times$ Condition ( $P<0.0001$ ), with Tukey corrections revealing significantly reduced magnitudes of reaction torque in the Rf condition compared with the other three experimental conditions, as well as significant differences between the remaining pairwise comparisons, indicating consistent effects of radius and friction properties on the torque exerted about the rung (Fig. 4C; Table S1H). In the Rf condition, reaction torques on the upper and lower rungs both approach zero, indicating that eccentric force application and/or moments achieved by grasping are severely limited by rungs with a large radius and low surface friction (Rf).

### Free moment

The free moment about the bird's pitch axis ( $M_z'$ ) can counter (e.g. Fig. 1B) or exacerbate the gravitational pitching moment during climbing. Here, we considered only the effect of perpendicular horizontal forces ( $F_x$ ) on  $M_z'$ . Given that the climbing ladder is nearly vertical, there is only a small separation between  $F_y$  vectors on adjacent rungs and the effect of vertical force ( $F_y$ ) on  $M_z'$  is negligible. Because  $M_z'$  is determined by a force couple on adjacent rungs, it is defined only for a pair of rungs, rather than for each rung individually as reported for reaction force and torque. Across all conditions,  $M_z'$  was negative (Fig. 5A), opposing the gravitational pitching moment (Fig. 1B). The main effect Stride was significant ( $P<0.0001$ ) and  $M_z'$  had a significantly greater magnitude in the second stride of the climbing sequence than in the first. Across all conditions,  $M_z'$  was not sufficiently negative to counter the gravitational moment during the first climbing stride; however, this was compensated for in the second climbing stride with a more negative  $M_z'$ .

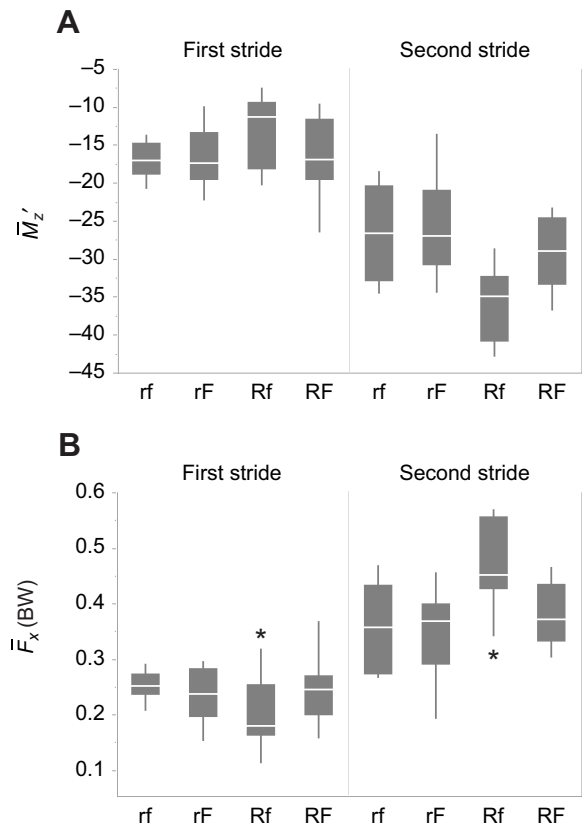


**Fig. 5. Mean free moments and horizontal force magnitudes for the first and second strides of the climbing sequence.** Mean free moment about the pitch axis ( $\bar{M}_z'$ ; A) and mean horizontal force magnitude ( $\bar{F}_x$ ; B) for upper and lower rungs over a full stride period. Force is in units of body weight (BW) and free moment is in units of body weight millimeters (BW mm). Condition: rf, small-radius, low-friction; rF, small-radius, high-friction; Rf, large-radius, low-friction; RF, large-radius, high-friction. \*Significant pairwise difference ( $P<0.05$ ) from other conditions (Table S1I). Stride: first, second.

### Magnitude of horizontal reaction force

The magnitude of  $M_z'$  depends only on the horizontal forces ( $F_x$ ) exerted on the lower and upper rungs because the vertical distance ( $S$ ) between the rungs of the experimental climbing ladder is fixed. A free moment is only achieved between points of contact when horizontal forces are in opposite directions: pulling inward from the upper rung and pushing outward from the lower rung to counter the gravitational moment. However, the magnitudes of those opposing horizontal forces may be mismatched, in which case the magnitude of  $M_z'$  is determined by the lesser of the two magnitudes. The greater the mismatch between horizontal force magnitudes, the lower the free moment for a given total horizontal force magnitude. For example, mean  $M_z'$  during the stride will be small when horizontal force magnitudes are frequently mismatched, whereas the average  $M_z'$  will be greatest when the horizontal force magnitudes are matched in every instance of the stride. Mean horizontal force magnitude is determined by averaging the absolute values of horizontal force on the lower and upper rungs (Table 2, Fig. 5B). The main effects Stride ( $P<0.0001$ ) and Condition ( $P=0.0005$ ) were highly significant, as was the interaction Stride $\times$ Condition ( $P<0.0001$ ). Tukey corrections showed significant pairwise differences between the Rf condition compared with the other three conditions (Fig. 5B; Table S1I). Horizontal force magnitude was smaller in the first stride and greater in the second stride of the

**Table 4. Standard major axis regression coefficients for mean free moment  $\bar{M}_z'$  on mean horizontal force magnitude  $|\bar{F}_x|$** 

Condition	<i>n</i>	SMA slope	<i>P</i> for slope >−92	<i>t</i> -statistic	<i>R</i> <sup>2</sup>
rf	20	−76.0	0.0031	−0.6264	0.94
rF6	24	−80.0	0.0005	−0.6593	0.97
Rf	19	−82.9	<0.0001	−0.6373	0.98
RF	20	−90.2	0.4214	−0.1904	0.99

*P* values are for the difference from a maximally effective slope of −92. SMA, standard major axis; rf, small-radius, low-friction; rF, small-radius, high-friction; Rf, large-radius, low-friction; RF, large-radius, high-friction.

Rf condition, again suggesting compensation in the second stride for insufficient  $\bar{M}_z'$  in the first stride.

### Efficacy of the free moment $\bar{M}_z'$

The free moment on the climbing ladder used in these experiments was determined by the perpendicular horizontal forces on an adjacent pair of rungs. When rung forces are opposite but not equal, the magnitude of the free moment is limited by the lesser of the two horizontal forces. To relate the magnitude of horizontal force to the free moment during a climbing stride, the absolute value of horizontal forces on the lower and upper rungs was averaged (Table 2). In the idealized case where  $F_x$  values on the lower and upper rungs are equal and opposite in every instance of the stride, all of the perpendicular horizontal force will contribute to the free moment and the slope of the line relating  $\bar{M}_z'$  to  $|\bar{F}_x|$  will equal the negative of the effective separation between rungs, taken to be  $S'=92$  mm. Hence, the efficacy with which the horizontal force produces a free moment is 100% when the regression of  $\bar{M}_z'$  on  $|\bar{F}_x|$  yields a slope of −92.

Comparing slopes of the lines relating  $\bar{M}_z'$  to  $|\bar{F}_x|$  across all four conditions shows the greatest efficacy of free moment on large-radius rungs: RF −90.2/−92 (98%) and Rf −82.9/−92 (90%) (Table 4); however, this should be interpreted cautiously because the actual separation between points of contact could be greater as a result of the larger radius of the rungs. The measured efficacy of free moment production on the small-radius rungs condition was: rF −80/−92 (87%) and rf −76/−92 (79%). To statistically compare these slopes with each other and with the maximally effective value, we used SMA regressions with the *smatr* package in R. Within the large-radius rungs, the high-friction rung condition showed significantly greater efficacy than the low-friction rung condition ( $P=0.013316$ ) and was not significantly different from the maximally effective value of −92 ( $P=0.42143$ ). This suggests that inadequate friction compromises the timing and/or magnitude of horizontal force couples required to achieve a free moment. Within the small radius rungs, efficacy did not increase significantly with greater friction ( $P=0.37818$ ). Small radius rungs also showed significantly lower efficacies than the maximal value of −92 (rf:  $P<0.0031$ , rF:  $P<0.0005$ ); however, comparisons with the large radius conditions should be made cautiously because of the noted potential for a greater actual separation between points of contact on thicker rungs.

### DISCUSSION

In this study, we measured 3D force and torque from individual rungs on a climbing ladder and used these data to analyze the dynamics of vertical climbing by green-cheeked conures. We found that (1) most of the vertical force for climbing is exerted by pulling upward from the upper rung rather than pushing upward from the lower rung, (2) reaction torque about the rung is in the wrong direction to resist the gravitational pitching moment that tends to

rotate the head away from the climbing surface, and (3) the gravitational pitching moment is resisted entirely by the free moment produced by opposing horizontal forces on separate rungs. This study represents the first dynamic analysis of an avian grasping climber and the first experimental measurement of free moments during arboreal locomotion on discrete rungs.

Like many quadrupedal arboreal specialists, conures use multiple contacts with overlapping durations (Fig. 3; Movies 1–3) to climb vertically and, in contrast to hopping climbers such as nuthatches, woodpeckers and treecreepers (Fujita et al., 2007, 2008; Norberg, 1986), do not show an aerial period. The gait sequence was led by the beak's initial contact on the upper rung, followed by the first and second foot on the upper rung. The tail contacts the lower rung as the second foot releases the lower rung to reach for the upper rung, underscoring the importance of the tail in maintaining the lower contact point of the force couple during progression from rung to rung (Fig. 1B). Although they are hopping rather than striding, woodpeckers and treecreepers also use tail contact to maintain a lower point of contact during vertical climbing on tree trunks (Fujita et al., 2007; Norberg, 1986). In our experiments, conures placed the point of the beak on top of the rung (like a grappling hook) rather than the more common behavior of grasping with the beak. During the first third of the stride, the beak is the sole contact point on the upper rung; hence, it provides the upper contact of the force couple until the first foot reaches the upper rung. The gravitational pitching moment is resisted by a free moment produced by the beak and feet during the first third of the stride and the tail and feet during the last third of the stride when the tail is the sole contact on the lower rung. These elements of the axial skeleton play a key role in pitch stabilization during climbing, so the neck–head–beak and the tail retrices may be called 'effective limbs' in the sense of Bertram (2016).

Throughout the climbing stride, substantially greater vertical force is exerted on the upper rung than on the lower rung. Across experimental conditions, about 80% of the total vertical force is due to pulling upward from the upper rung and the remaining 20% is due to pushing upward from the lower rung (Fig. 4A). This dominance of pulling is unexpected from the perspective of terrestrial limbs that push against the substrate and provides an important context for examining structure–function relationships in the hindlimbs, neck, head and beak of parrots. The dominance of upward pulling force could prove analogous to forelimb-dominated strategies posited for vertically climbing quadrupeds with relatively long forelimbs (Heinrich and Biknevicius, 1998; Johnson et al., 2015; Runestad, 1997). Hanna et al. (2017) showed that primates mostly push with their hindlimbs during vertical climbing.

Rung-axis torques were about an order of magnitude smaller than the free moments measured and were in the direction that would exacerbate the gravitational pitching moment, thus ruling out the torque strategy as a mechanism for pitch stability under the experimental rung conditions tested. We measured substantive reaction torque only on the upper rung and this torque, were it in response to a 'twisting' moment exerted by grasping feet, would tend to pitch the body in the same direction as the gravitational pitching moment. This contrasts with our *a priori* prediction that reaction torque might be due to a twisting action about the rung that would help resist the gravitational moment (Fig. 1A). Because it occurs only on the upper rung, it is possible that the torque measured at the rung might be an unintended consequence of upward pulling by a grasping foot and comparisons between experimental conditions support this possibility (Fig. 4; Table S1H). Little or no torque is exerted during climbing in the large-radius, low-friction



Rf condition and torque in the large-radius, high-friction Rf condition is significantly greater. If we allow that friction is limited by a smooth rung surface combined with a rung circumference too great for the foot to grasp completely, the torque about the rung would indeed approach zero. In the case of a foot that can exert no torque about the long-axis of the rung, reaction force that pulls the bird inward and upward toward the upper rung could only be achieved by a ‘hooking’ action of the foot. In other words, a frictionless hook can only produce a force vector that passes through the rung axis, whereas friction permits an eccentric line of action and a torque about the rung axis. Kinematic and electromyographic analyses are needed to test these ideas and to better understand the coordinated action of the hindlimb muscles to achieve an upward and inward pull.

The gravitational pitching moment is resisted entirely by the free moment during vertical climbing of conures, and this is achieved by opposing horizontal forces exerted on separate rungs. Free moments are produced, alternately, by force couples of the beak–foot, foot–foot and tail–foot acting on separate rungs (Fig. 1B). The gait pattern allows a free moment to be produced throughout most of the stride, as evidenced by the overlapping contacts on lower and upper rungs (Fig. 3; Movies 1–3). During the first third of the stride, a force couple is provided by the beak pulling inward on the upper rung and foot 2 pushing outward on the lower rung. For a brief period after departure of the beak, foot 1 pulls inward from the upper rung while foot 2 pushes outward from the lower rung, followed by a period of single foot support on the upper rung, which produces no free moment. During the last third of the stride, foot 1 followed by foot 2 pull inward on the upper rung while the tail pushes outward on the lower rung. By producing free moments to counter the gravitational moment throughout most of the stride, parrots can progress slowly in order to forage or change course without pitch perturbation. This contrasts with the faster and more ‘patterned’ climbing of nuthatches and woodpeckers, which tend to climb on tree trunks to canvas the surface of the substrate itself (Backhouse, 2009).

The magnitude of the mean free moment is statistically similar across all conditions, yet it is always greater in the second of the two strides measured. This disparity between strides shows that the gravitational pitching moment is not sufficiently resisted by the free moment during the first stride and that this imbalance is compensated for by a greater magnitude of mean free moment in the second stride. We introduce a concept of the efficacy by which horizontal forces produce a free moment – a metric determined by regression of mean free moment on the mean magnitude of horizontal force. Full efficacy would be achieved when horizontal forces are equal and opposite in every instance of the stride, representing only a force couple (i.e. there is no net horizontal force). In this idealized case, the regression of free moment on horizontal force magnitude would yield a slope with a magnitude equal to the vertical separation between contact points – a value taken to be  $S'=92$  mm in this study. Only the large-radius, high friction Rf rung condition resulted in efficacies that were statistically similar to the assumed maximum efficacy (96% of maximum; Table 4), whereas the large-radius, low friction Rf condition produced significantly lower efficacies (88% of maximum). Because a greater rung radius can alter the vertical spacing of contact points used by the birds, efficacy should be compared only between conditions with rungs of equal radius. Within small-radius rung conditions, friction did not increase efficacy significantly. Hence, it can be concluded that efficacy of the free moment is limited by the combination of low friction and the

inability of the foot to completely grasp the large-radius rung – again, suggesting that the foot is being used more like a hook in the Rf condition, and perhaps compromising control of the free moment. The concept of efficacy in producing free moments during vertical climbing may prove to be a useful approach in comparative studies where vertical rung spacing and rung radius are held constant or if the instantaneous center of pressure can be determined from an instrumented climbing surface.

While clearly ideal for grasping as a unit (Sustaita et al., 2013), the lengthened digits of parrots’ zygodactyl feet can also flex independently of each other (Carril et al., 2014) and seem well suited for a hook-like function when it is not possible to develop sufficient friction by fully grasping a branch, vine or other climbing surface. Our data demonstrate the ability of the conure’s hindlimb to pull the body inward and upward in the Rf condition, but kinematic analysis is required to reveal the mechanism by which this is achieved. For example, a purchase on the rung may be achieved by the grasping zygodactyl foot rotating in the yaw plane (i.e. about an axis perpendicular to the climbing plane) to dynamically wedge opposing pairs of digits against the top (digits II and III) and bottom (digits I and IV) of the climbing rung – which is conceptually supported by the fact that morphological modifications enable simultaneous flexion and adduction of digit II (Carril et al., 2014). It is important to note that parrots use their feet for a wide variety of both locomotor (climbing, hanging and perching: Bock and Miller, 1959; Forshaw and Knight, 2010) and ecological (food handling and tactile exploration of objects: Berman, 1984; Carril et al., 2014) functions, making their morphology and function subject to other evolutionary pressures.

#### Axial structures as ‘effective limbs’ during vertical climbing

Interpreting structure–function relationships of the head and tail as ‘effective limbs’ for vertical climbing is, of course, complicated by their functions in feeding and flight. The functional anatomy of the head and beak is usually interpreted in light of feeding. For example, the well-developed and robust craniofacial hinge and unique suborbital arch of parrots have been interpreted to function in seed crushing (e.g. Tokita, 2003). Likewise, the psittacine neck has not yet been evaluated from the perspective of climbing locomotion. Although all avian necks are highly flexible and similarly regionalized to form a characteristic S-shape, only three general shape variants have been identified, and none is unique to parrots (Terray et al., 2020). Among all birds, however, parrots have notably few cervical vertebrae: 10 in macaws, *Ara*; 11 in cockatoos, *Cacatua*; and 12 in Amazons, *Amazona*. Robustness of the craniofacial joint and relatively few cervical vertebrae might support the musculoskeletal functions of moving the body upward and pulling inward during vertical climbing of parrots.

The tail’s contribution during vertical climbing was unexpected, as parrots are not known to be classically tail-supported climbers (with the notable exception of the *Micropsitta* pygmy parrots: Forshaw and Knight, 2010). The tail contributed to the force couple during the last third of the stride by pushing against the lower rung to produce a reaction force away from the ladder. Without this final contact of an ‘effective limb’ on the lower rung, a free moment would not be possible once the second foot is released from the lower rung to reach for the upper rung.

Avian tail movement is controlled largely by axial muscles inserting on the pygostyle. Pygostyle morphology correlates with ecology in some lineages of swimming birds, seemingly as a result of the tail’s function as a rudder (Felice and O’Connor, 2014). In woodpeckers, enlargement of the pygostyle and stiffening of the

retices seems to have facilitated the development of large body size in several genera of woodpeckers (Manegold and Toepfer, 2013). A relatively large pygostyle has been hypothesized as part of suite characters associated with arboreal locomotion in fossil parrots (Ksepka and Clarke, 2012; Ksepka et al., 2011) but pygostyle morphology is not well studied in extant parrots. Given the function of the conure's tail in force couple-mediated vertical climbing and the diversity of psittacine climbing styles, including tail-supported trunk climbers, comparative studies might show the size and/or shape of the pygostyle to be functional osteological correlates of arboreal locomotion.

For parrots in particular, there may be more specific ecological pressures for mechanical involvement of the tail in some climbing contexts. Many New World parrots cling to vertical or near-vertical substrates with low surface texture while feeding at clay licks, and species exhibit variation in tail morphology and substrate use during this behavior (L.L.R., personal observation); while this functional interpretation of tail use is speculative – and the ecological significance of clay-lick use is uncertain (Lee et al., 2010) – further examination of tail properties could open up avenues for ecological, life history and evolutionary research. Although the specifics of rectrix morphology and function are understudied from virtually all angles except those that pertain to the tail's use as an airfoil (but see Tubaro et al., 2002), they could prove to be key drivers of functional, morphological and ecological diversity observed within and between avian taxa.

#### Acknowledgements

We thank Kit C. Knight for help with data collection and Larry Troyan for identifying kinematic time markers.

#### Competing interests

The authors declare no competing or financial interests.

#### Author contributions

Conceptualization: L.L.R., C.J.B., D.V.L.; Methodology: L.L.R., C.J.B., D.V.L.; Software: D.V.L.; Formal analysis: L.L.R., D.V.L.; Investigation: L.L.R., M.R.I., A.M.C., D.V.L.; Resources: L.L.R., D.V.L.; Data curation: L.L.R., M.R.I., D.V.L.; Writing - original draft: L.L.R.; Writing - review & editing: L.L.R., D.R.C., F.G., M.R.I., A.M.C., D.V.L.; Visualization: L.L.R., C.J.B., D.V.L.; Supervision: D.R.C., F.G., D.V.L.; Project administration: L.L.R., A.M.C., D.V.L.; Funding acquisition: L.L.R., D.V.L.

#### Funding

Funding was provided by the National Science Foundation (grant no. 0840950 to D.V.L.; and 041233 and GRFP-1256065 to L.L.R.).

#### Data availability

Data are available from the Dryad digital repository (Carrier et al., 2021): doi:10.5061/dryad.xgxd254hr

#### References

- Autumn, K., Hsieh, S. T., Dudek, D. M., Chen, J., Chitaphan, C. and Full, R. J.** (2006). Dynamics of geckos running vertically. *J. Exp. Biol.* **209**, 260-272. doi:10.1242/jeb.01980
- Backman, F.** (2009). *Woodpeckers of North America*, pp. 11-17. Firefly Books.
- Bertram, S. L.** (1984). The hindlimb musculature of the white-fronted Amazon (*Amazona albifrons*, Psittaciformes). *Auk* **101**, 74-92. doi:10.1093/auk/101.1.74
- Bertram, J. E. A.** (2016). *Understanding Mammalian Locomotion* (ed. J. E. A. Bertram), pp. 83-92. Hoboken, NJ: John Wiley & Sons, Inc.
- Biewener, A. A.** (2003). *Animal Locomotion*. Oxford University Press.
- Bock, W. J. and Miller, W. D.** (1959). The scansorial foot of the woodpeckers, with comments on the evolution of perching and climbing feet in birds. *Am. Mus. Novit.* **1931**, 9-45.
- Bock, W. J. and Winkler, H.** (1978). Mechanical analysis of the external forces on climbing mammals. *Zoomorphologie* **91**, 49-61. doi:10.1007/BF00994153
- Carrascal, L. M., Moreno, E. and Telleria, J. L.** (1990). Ecomorphological relationships in a group of insectivorous birds of temperate forests in winter. *Holarct. Ecol.* **13**, 105-111.
- Carrier, D., Reader, L. and Lee, D.** (2021). Climbing parrots achieve pitch stability using axial-appendicular force couples. *Dryad, Dataset*. doi:10.5061/dryad.xgxd254hr
- Carril, J., Mosto, M. C. and Picasso, M. B. J.** (2014). Hindlimb myology of the monk parakeet (*Aves*, Psittaciformes). *J. Morphol.* **275**, 732-744. doi:10.1002/jmor.20253
- Cartmill, M.** (1985). Climbing. In *Functional Vertebrate Morphology* (ed. M. Hildebrand, D. M. Bramble, K. F. Liem and D. B. Wake), pp. 73-88. Cambridge, MA: Belknap Press of Harvard University Press.
- Clemente, C. J., Withers, P. C., Thompson, G. G. and Lloyd, D.** (2013). Lizard tricks: Overcoming conflicting requirements of speed versus climbing ability by altering biomechanics of the lizard stride. *J. Exp. Biol.* **216**, 3854-3862.
- Dunning, J. B.** (2008). *CRC Handbook of Avian Body Masses*, 2nd edn. CRC Press.
- Felice, R. N. and O'Connor, P. M.** (2014). Ecology and caudal skeletal morphology in birds: the convergent evolution of pygostyle shape in underwater foraging taxa. *PLoS ONE* **9**, e89737. doi:10.1371/journal.pone.0089737
- Fischer, M. S., Krause, C. and Lilje, K. E.** (2010). Evolution of chameleon locomotion, or how to become arboreal as a reptile. *Zoology* **113**, 67-74. doi:10.1016/j.zool.2009.07.001
- Forshaw, J. M. and Knight, F.** (2010). *Parrots of the World*. Princeton University Press.
- Fujita, M., Kawakami, K. and Higuchi, H.** (2007). Hopping and climbing gait of Japanese Pygmy Woodpeckers (*Picoides kizuki*). *Comp. Biochem. Physiol. A. Mol. Integr. Physiol.* **148**, 802-810. doi:10.1016/j.cbpa.2006.06.048
- Fujita, M., Kawakami, K., Moriguchi, S. and Higuchi, H.** (2008). Locomotion of the Eurasian nuthatch on vertical and horizontal substrates. *J. Zool.* **274**, 357-366. doi:10.1111/j.1469-7998.2007.00395.x
- Godfrey, L. R., Sutherland, M. R., Paine, R. R., Williams, F. L., Boy, D. S. and Vuillaume-Randriamanantena, M.** (1995). Limb joint surface areas and their ratios in Malagasy lemurs and other mammals. *Am. J. Phys. Anthropol.* **97**, 11-36. doi:10.1002/ajpa.1330970103
- Goldman, D. I., Chen, T. S., Dudek, D. M. and Full, R. J.** (2006). Dynamics of rapid vertical climbing in cockroaches reveals a template. *J. Exp. Biol.* **209**, 2990-3000. doi:10.1242/jeb.02322
- Hagey, T. J., Harte, S., Vickers, M., Harmon, L. J. and Schwarzkopf, L.** (2017). There's more than one way to climb a tree: Limb length and microhabitat use in lizards with toe pads. *PLoS ONE* **12**, 1-17. doi:10.1371/journal.pone.0184641
- Hanna, J. B., Granatosky, M. C., Rana, P. and Schmitt, D.** (2017). The evolution of vertical climbing in primates: evidence from reaction forces. *J. Exp. Biol.* **220**, 3039-3052. doi:10.1242/jeb.157628
- Heinrich, R. E. and Biknevicius, A. R.** (1998). Skeletal allometry and interlimb scaling patterns in mustelid carnivores. *J. Morphol.* **235**, 121-134. doi:10.1002/(SICI)1097-4687(199802)235:2<121::AID-JMOR3>3.0.CO;2-C
- Hildebrand, M. and Goslow, G.** (2001). Climbing. In *Analysis of Vertebrate Structure*, pp. 519-546. New York City: John Wiley & Sons.
- Holden, J. P. and Cavanagh, P. R.** (1991). The free moment of ground reaction in distance running and its changes with pronation. *J. Biomech.* **24**, 887-897. doi:10.1016/0021-9290(91)90167-L
- Hunt, K. D., Cant, J. G. H., Gebo, D. L., Rose, M. D., Walker, S. E. and Youlatos, D.** (1996). Standardized descriptions of primate locomotor and postural modes. *Primates* **37**, 363-387. doi:10.1007/BF02381373
- Johnson, L. E., Hanna, J. and Schmitt, D.** (2015). Single-limb force data for two lemur species while vertically clinging. *Am. J. Phys. Anthropol.* **158**, 463-474. doi:10.1002/ajpa.22803
- Jusufi, A., Goldman, D. I., Revzen, S. and Full, R. J.** (2008). Active tails enhance arboreal acrobatics in geckos. *Proc. Natl. Acad. Sci. U. S. A.* **105**, 4215-4219. doi:10.1073/pnas.0711944105
- Ksepka, D. T. and Clarke, J. A.** (2012). A new stem parrot from the Green River Formation and the complex evolution of the grasping foot in Pan-Psittaciformes. *J. Vertebr. Paleontol.* **32**, 395-406. doi:10.1080/02724634.2012.641704
- Ksepka, D. T., Clarke, J. A. and Grande, L.** (2011). Stem parrots (*Aves*, Halcyornithidae) from the Green River Formation and a combined phylogeny of Pan-Psittaciformes. *J. Paleontol.* **85**, 835-852. doi:10.1666/10-108.1
- Lammers, A. R.** (2009). Mechanics of generating friction during locomotion on rough and smooth arboreal trackways. *J. Exp. Biol.* **212**, 1163-1169. doi:10.1242/jeb.027938
- Lammers, A. R. and Biknevicius, A. R.** (2004). The biodynamics of arboreal locomotion: The effects of substrate diameter on locomotor kinetics in the gray short-tailed opossum (*Monodelphis domestica*). *J. Exp. Biol.* **207**, 4325-4336. doi:10.1242/jeb.01231
- Lammers, A. R. and Gauntner, T.** (2008a). Mechanics of torque generation during quadrupedal arboreal locomotion. *J. Biomech.* **41**, 2388-2395. doi:10.1016/j.jbiomech.2008.05.038
- Lammers, A. R. and Gauntner, T.** (2008b). Erratum to "Mechanics of torque generation during quadrupedal arboreal locomotion". *J. Biomech.* **41**, 3295-3296. doi:10.1016/j.jbiomech.2008.08.011
- Lammers, A. R. and Sufka, K. M.** (2013). Turning the corner in quadrupedal arboreal locomotion: kinetics of changing direction while running in the siberian

- chipmunk (*Tamias sibiricus*). *J. Exp. Zool. Part A Ecol. Genet. Physiol.* **319**, 99-112. doi:10.1002/jez.1775
- Lee, A. T. K., Kumar, S., Brightsmith, D. J. and Marsden, S. J.** (2010). Parrot claylick distribution in South America: do patterns of "where" help answer the question "why"? *Ecography (Cop.)*, **33**, 503-513. doi:10.1111/j.1600-0587.2009.05878.x
- Manegold, A. and Toepfer, T.** (2013). The systematic position of *Hemicircus* and the stepwise evolution of adaptations for drilling, tapping and climbing up in true woodpeckers (Picinae, Picidae). *J. Zool. Syst. Evol. Res.* **51**, 72-82. doi:10.1111/jzs.12000
- Moreno, E. and Carrascal, L. M.** (1993). Leg morphology and feeding postures in four *Parus* species: an experimental ecomorphological approach. *Ecology* **74**, 2037-2044. doi:10.2307/1940849
- Norberg, R.** (1986). Treecreeper climbing: mechanics, energetics, and structural adaptations. *Ornis Scand* **17**, 191-209.
- Richardson, F.** (1942). Adaptive modifications for tree-trunk foraging in birds. *Univ. Calif. Publ. Zool.* **46**, 317-368.
- Runestad, J. A.** (1997). Postcranial adaptations for climbing in Loridae (Primates). *J. Zool.* **242**, 261-290. doi:10.1111/j.1469-7998.1997.tb05801.x
- Shapiro, L. J. and Young, J. W.** (2012). Erratum: Kinematics of quadrupedal locomotion in sugar gliders (*Petaurus breviceps*): Effects of age and substrate size (Journal of Experimental Biology (2012) 215 (480-496)). *J. Exp. Biol.* **215**, 4049. doi:10.1242/jeb.081224
- Spring, L. W.** (1965). Climbing and pecking adaptations in some North American woodpeckers. *Condor* **67**, 457-488. doi:10.2307/1365612
- Stoessel, A., Kilbourne, B. M. and Fischer, M. S.** (2013). Morphological integration versus ecological plasticity in the avian pelvic limb skeleton. *J. Morphol.* **274**, 483-495. doi:10.1002/jmor.20109
- Sustaita, D., Pouydebat, E., Manzano, A., Abdala, V., Hertel, F. and Herrel, A.** (2013). Getting a grip on tetrapod grasping: form, function, and evolution. *Biol. Rev. Camb. Philos. Soc.* **88**, 380-405. doi:10.1111/brv.12010
- Terray, L., Plateau, O., Abourachid, A., Böhmer, C., Delapré, A., de la Bernardie, X. and Cornette, R.** (2020). Modularity of the Neck in Birds (*Aves*). *Evol. Biol.* **47**, 97-110. doi:10.1007/s11692-020-09495-w
- Tokita, M.** (2003). The skull development of parrots with special reference to the emergence of a morphologically unique cranio-facial hinge. *Zool Sci.* **20**, 749-758. doi:10.2108/zsj.20.749
- Tubaro, P. L., Lijtmaer, D. A. and Palacios, M. G.** (2002). Adaptive modification of tail structure in relation to body mass and buckling in woodcreepers. *Am. Ornithol. Soc.* **104**, 281-296.
- Tulli, M. J., Abdala, V. and Cruz, F. B.** (2011). Relationships among morphology, clinging performance and habitat use in Liolaemini lizards. *J. Evol. Biol.* **24**, 843-855. doi:10.1111/j.1420-9101.2010.02218.x
- Zaaf, A., Van Damme, R., Herrel, A. and Aerts, P.** (2001a). Limb joint kinematics during vertical climbing and level running in a specialist climber: Gekko gekko Linneus, 1758 (Lacertilia: Gekkonidae). **131**, 173-182.
- Zaaf, A., Van Damme, R., Herrel, A. and Aerts, P.** (2001b). Spatio-temporal gait characteristics of level and vertical locomotion in a ground-dwelling and a climbing gekko. *J. Exp. Biol.* **204**, 1233-1246. doi:10.1242/jeb.204.7.1233
- Zeffer, A. and Norberg, U. M.** (2003). Leg morphology and locomotion in birds: requirements for force and speed during ankle flexion. *J. Exp. Biol.* **206**, 1085-1097. doi:10.1242/jeb.00208
- Zeffer, A., Christoffer Johansson, L. and Marmebro, Å.** (2003). Functional correlation between habitat use and leg morphology in birds (*Aves*). *Biol. J. Linnean Soc.* **79**, 461-484. doi:10.1046/J.1095-8312.2003.00200.X

**Table S1.** Pairwise comparisons by Tukey HSD are reported for vertical climbing parameters having a significant main effect of *CONDITION*. Bold indicates significant difference ( $P < 0.05$ ). Any significant interaction of *STRIDE* or *RUNG* with *CONDITION* is included. (*CONDITION*: rf = small-radius, low-friction; rF = small-radius, high-friction; Rf = large-radius, low-friction; RF = large-radius, high-friction) (*STRIDE*: first, second) (*RUNG*: lower, upper, both)

Table S1A - Pairwise comparisons of stride period (s)  
(Tukey-Kramer adjusted DF = 60.4)

Stride	Condition 1	Condition 2	Difference	Std Error	t Ratio	P
First	rF	Rf	-0.722164	0.0868402	-8.32	<b>&lt;.0001*</b>
First	rF	RF	-0.086835	0.0749563	-1.16	0.9404
First	rF	rf	0.164619	0.0794196	2.07	0.4438
First	Rf	RF	0.635329	0.0852285	7.45	<b>&lt;.0001*</b>
First	Rf	rf	0.886782	0.0897164	9.88	<b>&lt;.0001*</b>
First	RF	rf	0.251453	0.0771706	3.26	<b>0.0366*</b>
Second	rF	Rf	-0.196399	0.0825986	-2.38	0.2710
Second	rF	RF	0.017329	0.0722342	0.24	1.0000
Second	rF	rf	0.045372	0.0708497	0.64	0.9981
Second	Rf	RF	0.213728	0.0862296	2.48	0.2245
Second	Rf	rf	0.241771	0.0858061	2.82	0.1098
Second	RF	rf	0.028043	0.0751164	0.37	0.9999

Table S1B - Pairwise comparisons of duty factor for the beak  
(Tukey-Kramer adjusted DF = 60.4)

Condition 1	Condition 2	Difference	Std Error	t Ratio	P
rF	Rf	-0.248311	0.0290240	-8.56	<b>&lt;.0001*</b>
rF	RF	-0.060521	0.0252820	-2.39	0.0891
rF	rf	-0.017560	0.0261210	-0.67	0.9072
Rf	RF	0.187790	0.0297826	6.31	<b>&lt;.0001*</b>
Rf	rf	0.230751	0.0308970	7.47	<b>&lt;.0001*</b>
RF	rf	0.042961	0.0263022	1.63	0.3679

Table S1C - Pairwise comparisons of duty factor for the first foot  
(Tukey-Kramer adjusted DF = 60.4)

Stride	Condition 1	Condition 2	Difference	Std Error	t Ratio	P
First	rF	Rf	-0.065395	0.0420117	-1.56	0.7735
First	rF	RF	-0.012736	0.0362283	-0.35	1.0000
First	rF	rf	-0.019478	0.0383929	-0.51	0.9996
First	Rf	RF	0.052659	0.0412388	1.28	0.9038
First	Rf	rf	0.045917	0.0434378	1.06	0.9631
First	RF	rf	-0.006743	0.0372866	-0.18	1.0000
Second	rF	Rf	-0.203240	0.0399766	-5.08	<b>0.0001*</b>
Second	rF	RF	-0.159807	0.0349263	-4.58	<b>0.0006*</b>
Second	rF	rf	-0.092867	0.0342897	-2.71	0.1401
Second	Rf	RF	0.043433	0.0416898	1.04	0.9659
Second	Rf	rf	0.110373	0.0415524	2.66	0.1567
Second	RF	rf	0.066940	0.0363130	1.84	0.5938

Table S1D - Pairwise comparisons of duty factor for the second foot  
(Tukey-Kramer adjusted DF = 60.2)

Stride	Condition 1	Condition 2	Difference	Std Error	t Ratio	P
First	rF	Rf	0.056021	0.0426933	1.31	0.8907
First	rF	RF	-0.012584	0.0368508	-0.34	1.0000
First	rF	rf	-0.018938	0.0390449	-0.49	0.9997
First	Rf	RF	-0.068605	0.0419009	-1.64	0.7261
First	Rf	rf	-0.074959	0.0441071	-1.70	0.6875
First	RF	rf	-0.006354	0.0379398	-0.17	1.0000
Second	rF	Rf	-0.211914	0.0406064	-5.22	<b>&lt;.0001*</b>
Second	rF	RF	-0.155981	0.0355125	-4.39	<b>0.0011*</b>
Second	rF	rf	-0.078794	0.0348319	-2.26	0.3313
Second	Rf	RF	0.055933	0.0423928	1.32	0.8879
Second	Rf	rf	0.133120	0.0421831	3.16	<b>0.0480*</b>
Second	RF	rf	0.077187	0.0369295	2.09	0.4329

Table S1E - Pairwise comparisons of the second foot's contact phase  
(Tukey-Kramer adjusted DF = 60.9)

Condition 1	Condition 2	Difference	Std Error	t Ratio	P
rF	Rf	0.252763	0.0370439	6.82	<b>&lt;.0001*</b>
rF	RF	0.035186	0.0320996	1.10	0.6932
rF	rf	-0.027823	0.0333866	-0.83	0.8384
Rf	RF	-0.217577	0.0381491	-5.70	<b>&lt;.0001*</b>
Rf	rf	-0.280587	0.0400239	-7.01	<b>&lt;.0001*</b>
RF	rf	-0.063009	0.0334740	-1.88	0.2463

Table S1F - Pairwise comparisons of the tail's contact phase  
(Tukey-Kramer adjusted DF = 59.1)

Condition 1	Condition 2	Difference	Std Error	t Ratio	P
rF	Rf	0.115588	0.0299816	3.86	<b>0.0016*</b>
rF	RF	0.040688	0.0258487	1.57	0.4011
rF	rf	0.008780	0.0267135	0.33	0.9876
Rf	RF	-0.074901	0.0306882	-2.44	0.0805
Rf	rf	-0.106809	0.0320683	-3.33	<b>0.0079*</b>
RF	rf	-0.031908	0.0269994	-1.18	0.6406

Table S1G - Pairwise comparisons of mean horizontal reaction force (BW)  
(Tukey-Kramer adjusted DF = 218.8)

Condition 1	Condition 2	Difference	Std Error	t Ratio	P
Rf	RF	0.029773	0.0100199	2.97	<b>0.0172*</b>
Rf	rF	0.028838	0.0096228	3.00	<b>0.0160*</b>
Rf	rf	0.026787	0.0103295	2.59	<b>0.0494*</b>
RF	rF	-0.000935	0.0094913	-0.10	0.9997
RF	rf	-0.002986	0.0101125	-0.30	0.9910
rF	rf	-0.002051	0.0098186	-0.21	0.9968

Table S1H - Pairwise comparisons of mean torque about the rung (BW-mm)  
(Tukey-Kramer adjusted DF = 234.3)

Rung	Condition 1	Condition 2	Difference	Std Error	t Ratio	P
Lower	Rf	RF	-0.22398	0.357	-0.63	1.0000
Lower	Rf	rF	0.19567	0.343	0.57	1.0000
Lower	Rf	rf	0.04276	0.359	0.12	1.0000
Lower	RF	rF	0.41965	0.338	1.24	0.9849
Lower	RF	rf	0.26674	0.354	0.75	0.9998
Lower	rF	rf	-0.15291	0.340	-0.45	1.0000
Upper	Rf	RF	-5.43932	0.357	-15.22	<b>&lt;.0001*</b>
Upper	Rf	rF	-3.92509	0.343	-11.46	<b>&lt;.0001*</b>
Upper	Rf	rf	-1.82480	0.359	-5.08	<b>&lt;.0001*</b>
Upper	RF	rF	1.51424	0.338	4.48	<b>0.0007*</b>
Upper	RF	rf	3.61452	0.354	10.21	<b>&lt;.0001*</b>
Upper	rF	rf	2.10029	0.340	6.18	<b>&lt;.0001*</b>
Both	Rf	RF	-5.69954	0.357	-15.95	<b>&lt;.0001*</b>
Both	Rf	rF	-3.74818	0.343	-10.94	<b>&lt;.0001*</b>
Both	Rf	rf	-1.99880	0.359	-5.57	<b>&lt;.0001*</b>
Both	RF	rF	1.95136	0.338	5.78	<b>&lt;.0001*</b>
Both	RF	rf	3.70074	0.354	10.45	<b>&lt;.0001*</b>
Both	rF	rf	1.74938	0.340	5.14	<b>&lt;.0001*</b>

Table S11 - Pairwise comparisons of mean horizontal reaction force magnitude (BW)  
(Tukey-Kramer adjusted DF = 237.0)

Stride	Condition 1	Condition 2	Difference	Std Error	t Ratio	P
First	Rf	RF	-0.049763	0.0139	-3.59	<b>0.0094*</b>
First	Rf	rF	-0.035812	0.0133	-2.69	0.1295
First	Rf	rf	-0.051388	0.0143	-3.59	<b>0.0093*</b>
First	RF	rF	0.013951	0.0129	1.08	0.9603
First	RF	rf	-0.001624	0.0139	-0.12	1.0000
First	rF	rf	-0.015576	0.0134	-1.17	0.9409
Second	Rf	RF	0.088039	0.0135	6.53	<b>&lt;.0001*</b>
Second	Rf	rF	0.115141	0.0129	8.90	<b>&lt;.0001*</b>
Second	Rf	rf	0.091939	0.0133	6.92	<b>&lt;.0001*</b>
Second	RF	rF	0.027102	0.0129	2.10	0.4209
Second	RF	rf	0.003900	0.0133	0.29	1.0000
Second	rF	rf	-0.023202	0.0128	-1.81	0.6115



**Table S2.** ANOVA tables for Generalize Linear Models. Bold indicates significant difference ( $P < 0.05$ ). Interactions of *STRIDE* or *RUNG* with *CONDITION* are included when the main effect *CONDITION* is significant.

Table S2A - Stride period (s)

Source	DF	F-ratio	P
<b>CONDITION</b>	3	29.437566	<b>&lt;.0001*</b>
<b>STRIDE</b>	1	16.688627	<b>0.0001*</b>
<b>STRIDE*CONDITION</b>	3	9.9393819	<b>&lt;.0001*</b>

Table S2B - Duty factor - beak

Source	DF	F-ratio	P
<b>CONDITION</b>	3	26.915188	<b>&lt;.0001*</b>
<b>STRIDE</b>	1	17.086632	<b>0.0001*</b>
<b>STRIDE*CONDITION</b>	3	1.7134045	0.1738

Table S2C - Duty factor - first foot

Source	DF	F-ratio	P
<b>CONDITION</b>	3	8.2286137	<b>0.0001*</b>
<b>STRIDE</b>	1	3.3901782	0.0705
<b>STRIDE*CONDITION</b>	3	3.3487624	<b>0.0248*</b>

Table S2D - Duty factor - second foot

Source	DF	F-ratio	P
<b>CONDITION</b>	3	4.3306768	<b>0.0079*</b>
<b>STRIDE</b>	1	3.0489442	0.0859
<b>STRIDE*CONDITION</b>	3	7.6192276	<b>0.0002*</b>

Table S2E - Contact phase - first foot

Source	DF	F-ratio	P	
<b>CONDITION</b>		3	1.9422401	0.1322
<b>STRIDE</b>		1	10.615531	<b>0.0018*</b>
<b>STRIDE*CONDITION</b>		3	0.9692394	0.4132

Table S2F - Contact phase - second foot

Source	DF	F-ratio	P	
<b>CONDITION</b>		3	19.66907	<b>&lt;.0001*</b>
<b>STRIDE</b>		1	2.2845503	0.1359
<b>STRIDE*CONDITION</b>		3	2.622595	0.0586

Table S2G - Contact phase - tail

Source	DF	F-ratio	P	
<b>CONDITION</b>		3	5.4739247	<b>0.0022*</b>
<b>STRIDE</b>		1	110.92874	<b>&lt;.0001*</b>
<b>STRIDE*CONDITION</b>		3	0.5590183	0.6441

Table S2H - Mean vertical reaction force (BW)

Source	DF	F-ratio	P	
<b>CONDITION</b>		3	0.0708439	0.9754
<b>STRIDE</b>		1	0.3587231	0.5498
<b>RUNG</b>		2	2049.8507	<b>&lt;.0001*</b>

Table S2I - Mean horizontal reaction force (BW)

Source	DF	F-ratio	P
<b>CONDITION</b>	3	4.0513831	<b>0.0079*</b>
<b>STRIDE</b>	1	0.2976037	0.5859
<b>RUNG</b>	2	1024.1629	<b>&lt;.0001*</b>
<b>RUNG*CONDITION</b>	6	1.3761182	0.2250

Table S2J - Mean torque about the rung (BW-mm)

Source	DF	F-ratio	P
<b>CONDITION</b>	3	125.42119	<b>&lt;.0001*</b>
<b>STRIDE</b>	1	2.2613558	0.1340
<b>RUNG</b>	2	174.63331	<b>&lt;.0001*</b>
<b>RUNG*CONDITION</b>	6	29.476471	<b>&lt;.0001*</b>

Table S2K - Mean horizontal reaction force magnitude (BW)

Source	DF	F-ratio	P
<b>CONDITION</b>	3	6.1456635	<b>0.0005*</b>
<b>STRIDE</b>	1	602.06009	<b>&lt;.0001*</b>
<b>RUNG</b>	2	0.00503	0.9950
<b>STRIDE*CONDITION</b>	3	28.120576	<b>&lt;.0001*</b>

Table S2L - Mean free moment (BW-mm)

Source	DF	F-ratio	P
<b>CONDITION</b>	3	1.5922015	0.1982
<b>STRIDE</b>	1	148.17946	<b>&lt;.0001*</b>



**Movie 1.** Oblique horizontal view of a representative small-radius, low-friction trial



**Movie 2.** Oblique horizontal view of a representative large-radius, low-friction trial



**Movie 3.** Oblique horizontal view of a representative large-radius, high-friction trial